PAUL SCHERRER INSTITUT	SLS 2.0
Title Round beams in SLS 2.0 using coupling resonance	Document identification SLS2-KJ81-004-1
Author(s) J. Kallestrup	January 9, 2023

#### 1 Introduction

Operating the SLS 2.0 storage ring on the linear difference resonance  $Q_x - Q_y = p$  is an option for creating a round beam, here defined as the situation where the two transverse emittances are equal  $(\epsilon_x \approx \epsilon_y)$ . Several other options for creating round beams exist, see [1] and [2, 3] and references therein for two other examples. Through resonant betatron coupling, some of the horizontal action is transferred to the vertical plane, thereby giving equal emittances, where in particular the horizontal emittance is decreased while the vertical emittance is increased. On the resonance, the emittance will be given by

$$\epsilon_x = \epsilon_y = \epsilon_0 \left( \frac{J_x J_y}{J_x + J_y} \right),\tag{1}$$

where  $\epsilon_0$  is the natural emittance,  $J_x$  and  $J_y$  are the horizontal- and vertical damping partition numbers, respectively. The smaller horizontal emittance can potentially improve the brightness and coherent faction for beamlines producing photons in the  $\leq 1 \, \text{keV}$  region, while the much larger vertical emittance significantly improves Touschek lifetime, with the caveat that the lifetime might be limited by losses on vertical physical apertures.

This note presents a few simulations of the beam dynamics in the SLS 2.0 storage ring while working on the coupling resonance. The baseline lattice is B073 with 1.44 MeV total RF voltage. All computations are made using Accelerator Toolbox (AT) [4, 5]<sup>1</sup>, without collimators, insertion devices or intra-beam scattering. The natural emittance of B073 is 148 pm rad, the tunes are [39.37, 15.22] and the horizontal and vertical damping partition numbers are, respectively,  $J_x = 1.855$  and  $J_y = 1.000$ . The resonant working point is selected to be [39.22, 15.22].

#### 1.1 Coupling creation

The strength of the transverse coupling is conveniently quantified by the transverse coupling coefficient is [6]:

$$|C^{-}| = \frac{1}{2\pi} \oint k_s(s) \sqrt{\beta_x(s)\beta_y(s)} ds, \qquad (2)$$

where  $k_s(s)$  is the normalized skew quadrupole strength. |C| corresponds to the size of the linear difference resonance stop-band.

The coupling in the studies of this document is generated using the skew quadrupole coils on the harmonic octupole magnets (oxx, oxy and oyy); this choice is made in order to have the coupling source distributed to 72 locations to minimize beta-beating and avoid vertical dispersion.

<sup>&</sup>lt;sup>1</sup>A discrepancy between AT and tracy in terms of lifetime is observed; with the nominal working point AT yields lower lifetimes. This is not considered an issue since good momentum aperture can be recovered by optimization in AT specifically, and so the discrepancies between AT and tracy are considered to stem from the codes.

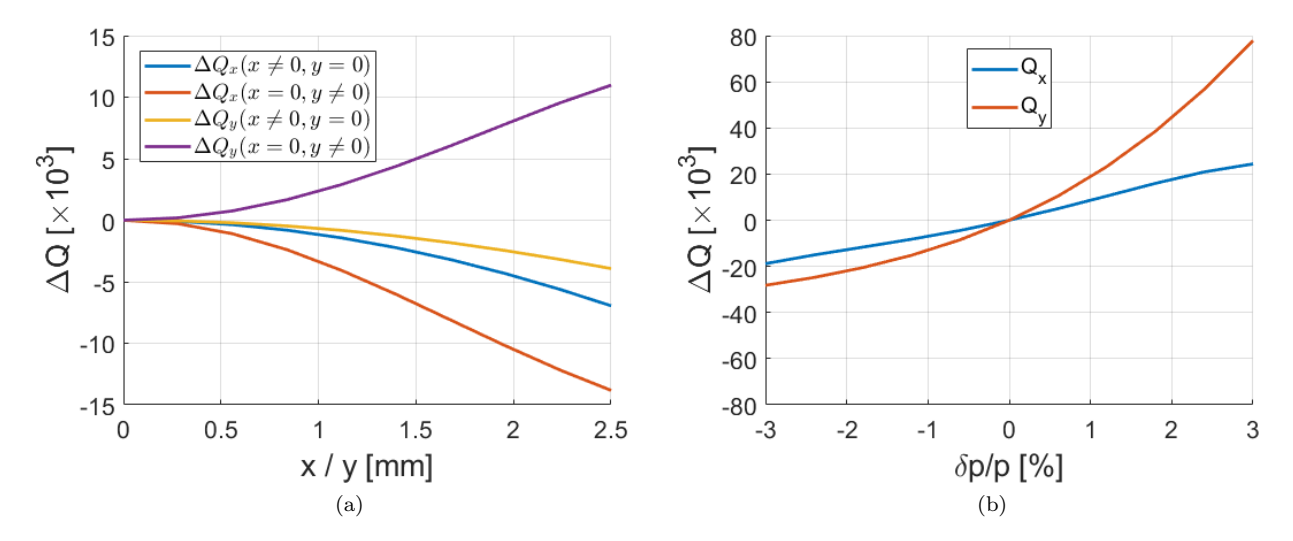


Figure 1: SLS 2.0 B073 lattice tune shifts a) with amplitude at the exit of the thin septum, b) with energy offset.

For the emittance sharing to be effective, it must be ensured that all particles experience the resonant coupling, i.e., all particles must be within the resonance stop-band. In other words, the tune-footprint, stemming from Amplitude Dependent Tune Shift (ADTS) and Chromatic Tune Shift (CTS) of the equilibrium bunch should be smaller than |C|. The ADTS and CTS for the SLS 2.0 lattice (computed in AT) is shown in Fig. 1. The relevant amplitude region to evaluate for ADTS is  $\pm 3\sigma$  of the beam size. The natural emittance of 148 pm rad is assumed in both planes since the full horizontal action can transfer to the vertical direction. At the exit of the thin septum (where the ADTS was evaluated in Fig. 1a), the  $3\sigma$  beam sizes are 175 µm and 88 µm for the horizontal and vertical plane, respectively, corresponding to amplitude-dependent tune shifts of  $|\Delta Q_x| \leq 8.9 \times 10^{-5}$  and  $|\Delta Q_y| \leq 3.3 \times 10^{-5}$ . Similarly, the chromatic tune shift is evaluated for particles with energy deviations of  $\pm 3\sigma_{\delta}$ , where  $\sigma_{\delta}$  is the energy spread of the bunch. Using Fig. 1b, it is found that  $-2.4 \times 10^{-3} \leq \Delta Q_x \leq 2.8 \times 10^{-3}$  and  $-4.6 \times 10^{-3} \leq \Delta Q_x \leq 5.8 \times 10^{-3}$ .

As mentioned, |C| must be larger than any value of  $\Delta Q$  that the particle may encounter to remain in resonance, and so  $|C| \approx 0.01$  is chosen as the default value for the simulations below.

# 2 Linear optics distortion

The tune is moved to the coupling resonance using all twelve straight sections without modifying the optics within the arcs. The optics is kept the same for all sextupoles regardless of straight section in order to avoid breaking symmetry. The tune shift therefore introduces a small beta-beating in the straight sections as shown with blue curves in Fig. 2.

The skew quadrupoles which are introduced in order couple the lattice will inevitably also perturb the linear optics. Prior to this study, it was expected that operating on the linear coupling resonance would lead to equalisation of not only the emittances but also remaining twiss functions. However, upon evaluation of the lattice envelope using Ohmi's envelope method (implemented in AT) [7] and subsequent confirmation using tracking including radiative effects, it was found that the linear optics of the machine is more or less unperturbed. The only weak perturbation stems from the skew quadrupoles themselves (i.e. a non-resonant effect), and this perturbation is minimized by distributing the coupling sources throughout the ring. Fig. 3 shows the analytic beta-functions for the coupled lattice together with tracking results in part of the machine. The tracking values are calculated from the covariance matrix of the output distributions after 40,000 turns in the machine and evaluated at source points. The disagreement between analytic calculations and tracking results are around  $\pm 1\%$ .

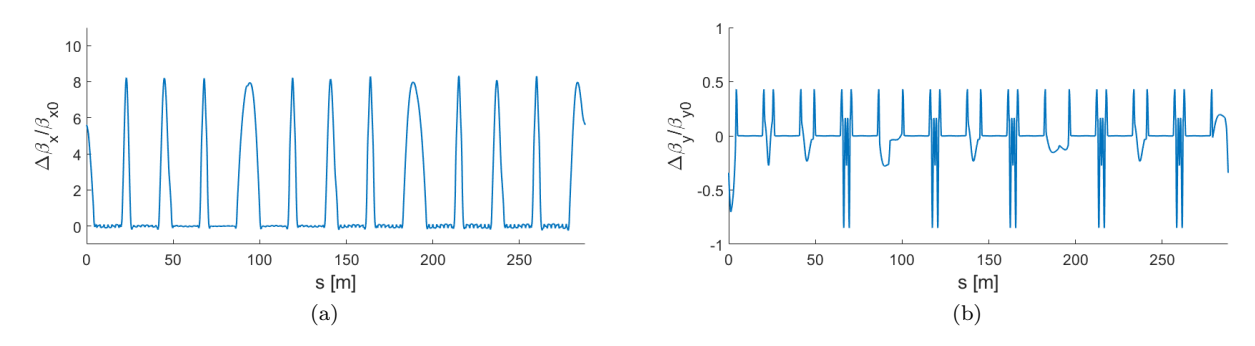


Figure 2: Beta-beating due to shift of working point to the coupling resonance before including coupling in the simulations.

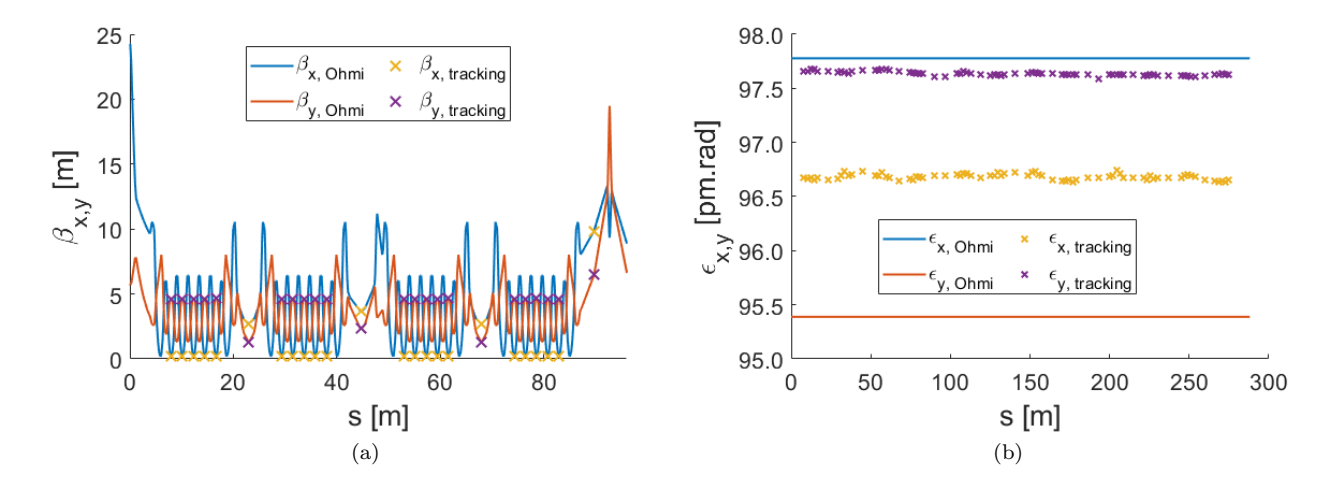


Figure 3:  $\beta$ -functions and emittances for the coupled lattice calculated using Ohmi's envelope technique and equivalents at source points obtained from equilibrium distributions after tracking 40,000 turns.

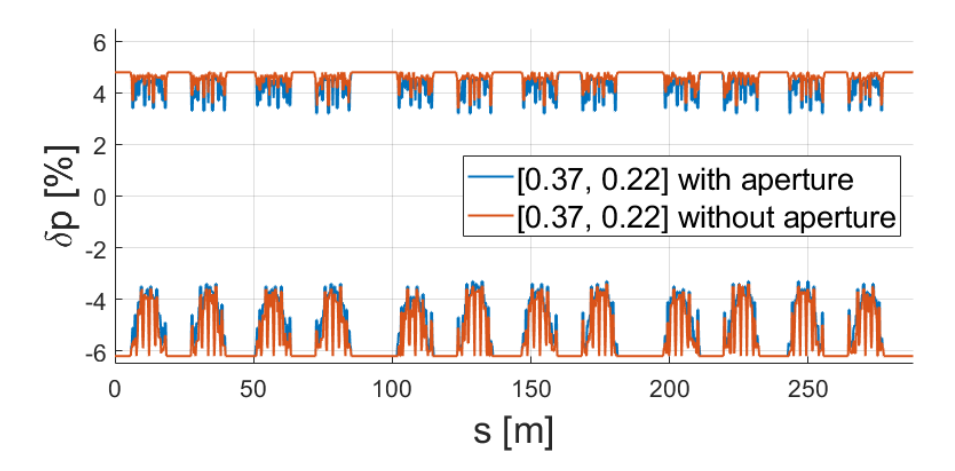


Figure 4: Momentum apertures for the nominal working point [39.37,15.22] with and without physical apertures (cases i) and ii), respectively).

## 3 Momentum aperture

The impact on momentum aperture is of the highest importance for round beam operation, since it plays a key role in the computation of the Touschek lifetime using the Piwinski formula. As a Touschek scattering event occurs, the particle will start to oscillate around the closed orbit that corresponds to the momentum deviation of the particle. This oscillation will remain horizontal under the assumption of no vertical dispersion (systematic or spurious) and no machine errors. However, vertical motion is created in the case of betatron coupling, and the full horizontal betatron amplitude will be transferred to the vertical plane if the working point is on the linear difference resonance. As a consequence, losses on narrow-gap insertion devices or vertical collimator may occur, thereby limiting the momentum aperture of the ring and, hence, the Touschek lifetime.

To explore the important mechanisms, we investigate the lattice in a few different cases:

- i) Nominal working point without aperture, without coupling
- ii) Nominal working point with aperture, without coupling
- iii) Resonant working point, without aperture, without coupling
- iv) Resonant working point, with aperture, without coupling
- v) Resonant working point, without aperture, with coupling
- vi) Resonant working point, with aperture, with coupling

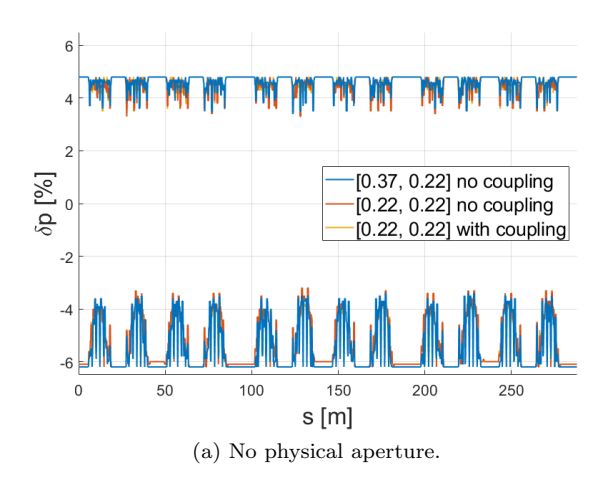
For the uncoupled cases, the Touschek lifetime is evaluated for "flat" design emittances  $\epsilon_x = 148 \,\mathrm{pm}\,\mathrm{rad}$  and  $\epsilon_y = 10 \,\mathrm{pm}\,\mathrm{rad}$ , while the coupled cases are evaluated for both flat- and round beam emittances, the latter found to be  $\epsilon_x = \epsilon_y = 96 \,\mathrm{pm}\,\mathrm{rad}$  through Eq. (1).

#### 3.1 Nominal working point

The purpose of the cases for the nominal working point, case i) and ii), is to access the affect of the machine aperture on the momentum aperture for the ideal lattice. As seen in Fig. 4, the physical apertures are reducing the momentum aperture in the arcs for the nominal working point. All losses are on horizontal apertures.

#### 3.2 Resonant working point with and without coupling

The next cases are simulations for the resonant working point with and without coupling sources.



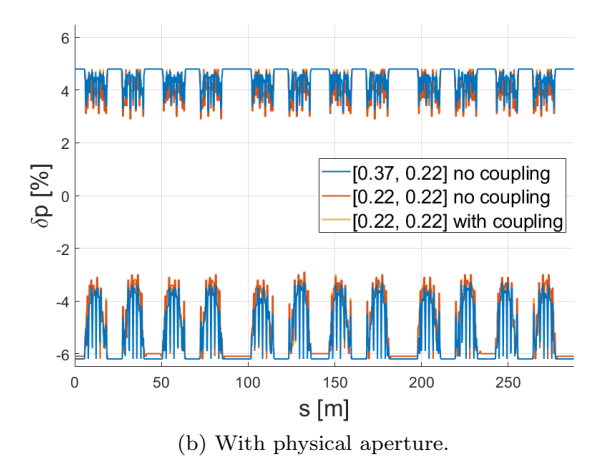


Figure 5: Momentum apertures for three cases a) without physical apertures and b) including physical apertures. Bracketed numbers indicate the fractional tunes of the lattices.

Table 1: Touschek lifetimes for various working points with/without coupling and with/without apertures.

	$Q_x$	$Q_y$	Has aperture?	$\epsilon_x$ [pm.rad]	$\epsilon_y$ [pm.rad]	C	$\tau_T$ [h]
Case i)	39.37	15.22	No	148	10	0	6.5
Case ii)	39.37	15.22	Yes	148	10	0	5.1
Case iii)	39.22	15.22	No	148	10	0	5.8
Case iv)	39.22	15.22	Yes	148	10	0	3.8
Case v) <sub>flat</sub>	39.22	15.22	No	148	10	0.086	5.9
Case v) <sub>round</sub>	39.22	15.22	No	96	96	0.086	17.8
Case iv) <sub>flat</sub>	39.22	15.22	Yes	148	10	0.086	3.9
Case vi) <sub>round</sub>	39.22	15.22	Yes	96	96	0.086	11.0

The momentum apertures for cases i), iii) and v) are compared in Fig. 5a to analyse the direct impact on dynamics, i.e., without aperture. Generally, there is not a great difference between the three cases. A simple comparison is made by evaluating the Touschek lifetime of the three cases using the flat-beam emittances; the Touschek lifetime for cases i), iii) and v) are  $6.5\,h$ ,  $5.8\,h$  and  $5.9\,h$ , respectively. This result shows that the new working point [39.22, 15.22] has slightly worse Touschek lifetime, but including the coupling sources does not lead to further reduction.

Next, the simulations are repeated but including the physical aperture model (not including collimators), i.e. cases ii), iv) and vi) from the list above. The momentum apertures are shown in Fig. 5b. By comparison with Fig. 5a, it is clear that the physical aperture is shrinking the momentum aperture. Yet again the Touschek lifetimes for the flat-beam emittances are used as a benchmark:  $5.1\,\mathrm{h}$ ,  $3.8\,\mathrm{h}$  and  $3.9\,\mathrm{h}$  for cases ii), iv) and vi), respectively, i.e. reduction factors of 1.27, 1.51 and 1.51, indicating that the resonant working point performs noticeably worse than the original lattice. Evaluation of case vi) for the round beam emittances lead to lifetimes of 17.8 h and 11.0 h without and with physical apertures, respectively. This means that a factor  $11.0\,\mathrm{h}/5.1\,\mathrm{h} = 2.16$  increase in Touschek lifetime can be achieved by operating on the coupling resonance.

# 4 Dynamic aperture

The impact on dynamic aperture (DA) of the change of working point and the distributed coupling is now evaluated with and without physical apertures. Fig. 6a shows the DA without apertures: shifting the working point does deteriorate the DA slightly, however, the introduction of coupling into the lattice does not affect the DA (since the yellow curve overlays the red curve). The impact of coupling is only seen when apertures are added (Fig. 6b): with the physical aperture, the DA is decreased slightly for [x, y] > [0, 0].

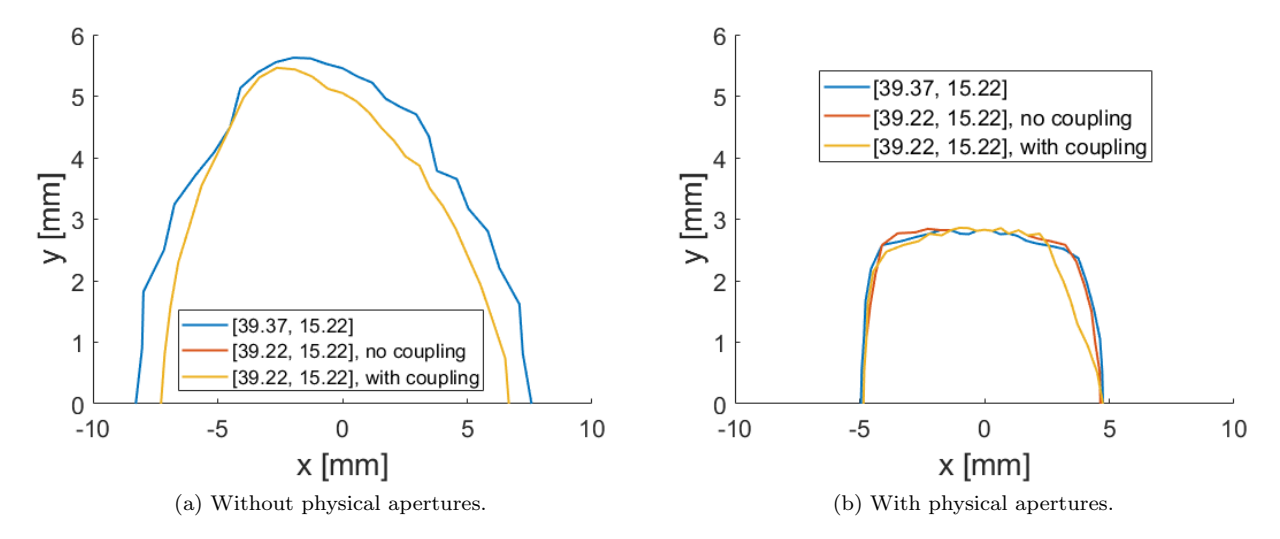


Figure 6: Dynamic apertures for the nominal working point (blue) and the coupling resonance working point (red and yellow). Left: without physical apertures. Right: with physical apertures.

## 5 Injection

The baseline injection scheme for SLS 2.0 is using the four-kicker bump to do standard off-axis injection, which will lead to horizontal injection beam oscillation amplitudes around 3 mm at the thin septum. Another foreseen scheme is single-bunch aperture sharing ("fast injection") which leads to oscillation amplitudes of both injected- and stored bunch to around 4 mm at the thin septum. The horizontal oscillations can convert into vertical motion due to the coupling, which potentially limits the usage of off-axis injection with round beams. Generally, assuming linear optics, the oscillation amplitude in the throughout the machine will scale as:

$$x(s) \propto x_0 \sqrt{\frac{\beta_x(s)}{\beta_{x0}}}.$$
 (3)

Since the coupling preserves action it means that the vertical oscillation due to a horizontal offset will scale as:

$$y(s) \propto x_0 \sqrt{\frac{\beta_y(s)}{\beta_{x0}}}$$
 (4)

The vertical motion will therefore be limited by the large horizontal beta-function at the injection straight. In Fig. 7 we have applied (4) to plot the  $3\sigma$  envelope for a beam injected with a 3 mm beam offset, i.e., four-kicker bump injection, assuming  $\epsilon_x = 2$  nm rad and  $\beta_x = 8.1$  m for the injected beam at the thin septum exit. Initial vertical beam-size is neglected. The large value of  $\beta_y$  at the long straight at the collimator location might be an issue

In Fig. 8 we show tracking results of the transverse phase spaces at the thin septum exit and the corresponding ellipses determined by linear optics. A vertical emittance of 12 nm rad was assumed. As is seen, both the horizontal- and vertical phase space agrees well with the predicted ellipses.

Initially, it was expected that the horizontal offset combined with the strong ADTS would mean that particles would be detuned away from the coupling resonance, so that no transfer of action between the transverse planes will happen until the beam has damped in amplitude. However, this effect is evidently small.

### 6 Discussion

In Section 3, no deterioration of the momentum aperture was found when the coupling sources were included in the simulation, indicating that the vertical physical aperture does not play a role in these simulations. Indeed,

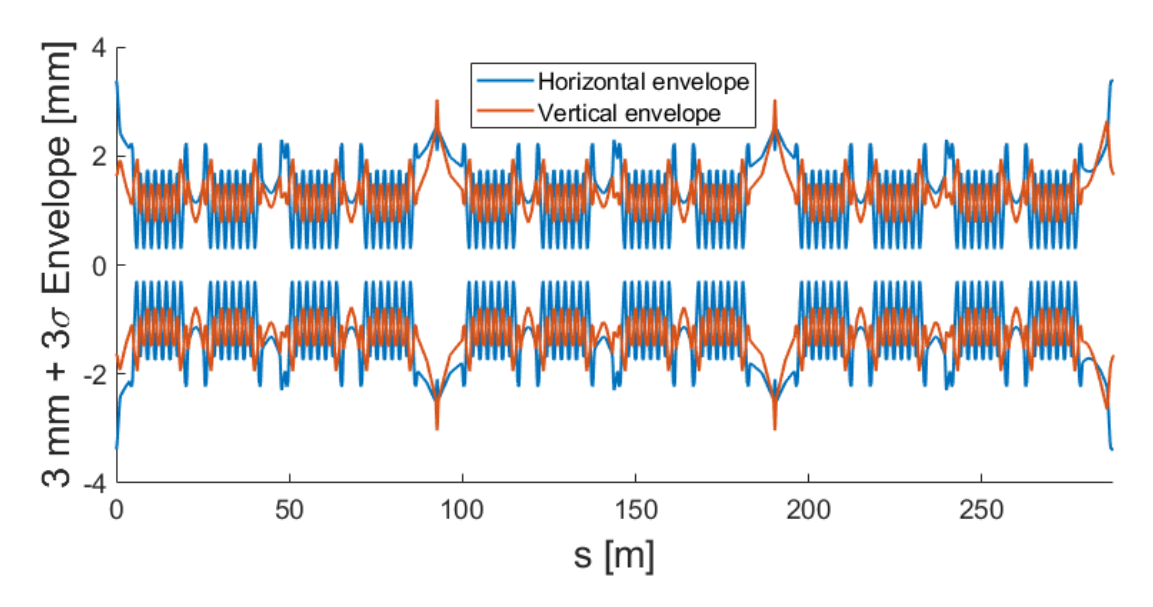


Figure 7:  $3\sigma$  envelopes of motion in horizontal- and vertical plane for a beam initially offset by 3 mm at the thin septum exit. The lattice is on the coupling resonance with a coupling coefficient of  $|C| \approx 0.01$ .

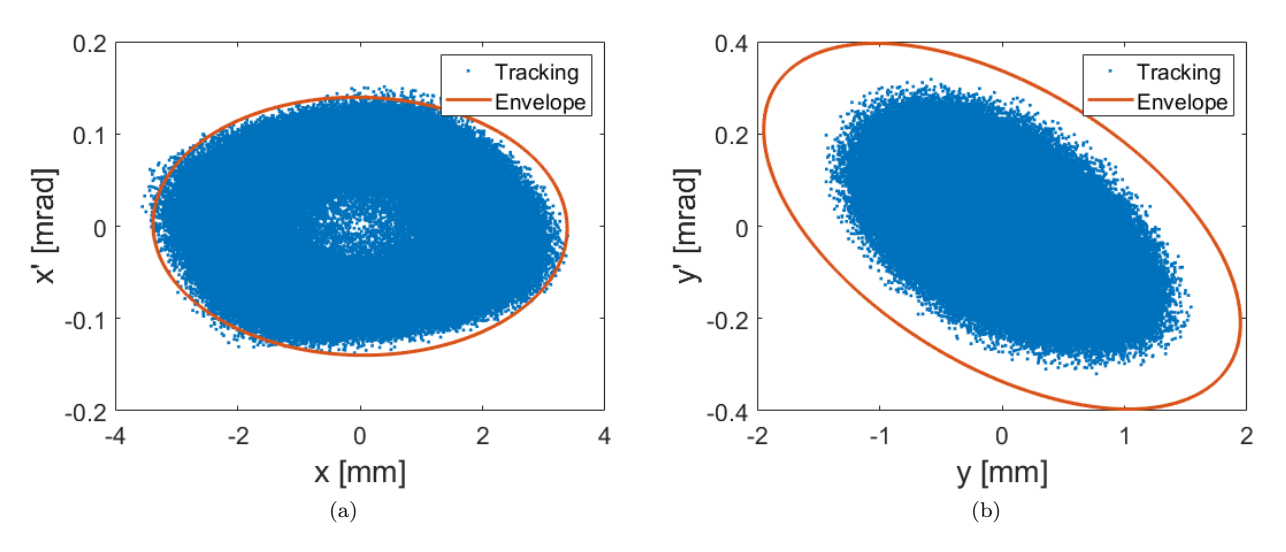


Figure 8: Transverse phase spaces of tracked particle distribution at the exit of the thin septum including coupling. Ellipses indicate the linear-optics-predicted envelopes at this location.

removing the only vertical aperture leads to exactly the same momentum aperture as the case where both horizontal and vertical apertures are included, showing that the horizontal aperture is the limitation.

Collimators were not included in the above simulations. The collimators are set in order to collect as many Touschek particles as possible without significant deterioration to machine performance. Adding the collimators will likely lead to a small reduction of momentum apertures. Additionally, they may limit the efficiency of off-axis injection.

It is well-known that there is a difference in the calculated momentum aperture between tracy and AT for the same magnet settings. The consequence is that AT reports lower lifetimes, which is also why the values in Table 1 are lower than the typical tracy lifetime of  $\approx 8\,\mathrm{h}$ . Since shifting the working point and adding coupling does not significantly alter the beam dynamics (see e.g. cases i), iii) and v) for the flat-beam emittance evaluation) we can assume that the same scaling of the Touschek lifetime when evaluating based on round-beam emittances; assuming an  $8\,\mathrm{h}$  lifetime we therefore expect an  $\approx 17\,\mathrm{h}$  lifetime when the beam is fully coupled including apertures.

### References

- [1] M. Aiba, M. Ehrlichman, and A. Streun, "Round beam operation in electron storage rings and generalisation of Mobius accelerator", IPAC'15, Richmond, USA, 2017, doi:10.18429/JACoW-IPAC2015-TUPJE045
- [2] P. Kuske and R. Görgen, "Vertical emittance control at BESSY", Proc. EPAC'02, Paris, France.
- [3] T. Nakamura, "x-y- coupling generation with ac/pulsed skew quadrupole and its application", Proc. 10th annual meeting of Particle Accelerator Society of Japan, p. 1123, 2013
- [4] A. Terebilo, "Accelerator Toolbox for MATLAB", SLAC-PUB-8732, May 2021
- [5] AT Collaboration, https://atcollab.github.io/at/
- [6] G. Guignard, "Betatron coupling and related impact of radiation", Phys. Rev. E 51, 6104, 1995.
- [7] K. Ohmi, K. Hirata, and K. Oide, "From the beam-envelope matrix to synchrotron-radiation integrals", Phys. Rev. E 49, 751, 1994